Langmuir

LETTER

pubs.acs.org/Langmuir

A Simple Approach for Local Contact Angle Determination on a Heterogeneous Surface

Jinbo Wu,[†] Mengying Zhang,[†] Xiang Wang,[†] Shunbo Li,[‡] and Weijia Wen*[,‡]

[†]NanoScience and NanoTechnology Program and [‡]Department of Physics, Hong Kong University of Science and Technology, Clear Water Bay, Kowloon, Hong Kong

ABSTRACT: We report a simple approach for measuring the local contact angle of liquids on a heterogeneous surface consisting of intersected hydrophobic and hydrophilic patch arrays, specifically by employing confocal microscopy and the addition of a very low concentration of Rhodamine-B (RB) (2×10^{-7} mol/L). Interestingly, RB at that concentration was found to be aggregated at the air−liquid and solid (hydrophobic patch only)−liquid interfaces, which helps us to distinguish the liquid and solid interfaces as well as hydrophobic and hydrophilic patches by their corresponding fluorescent intensities. From the measured local contact angles, the line tension can be easily derived and the value is found to be $(-2.06-1.53) \times 10^{-6}$ J/m.

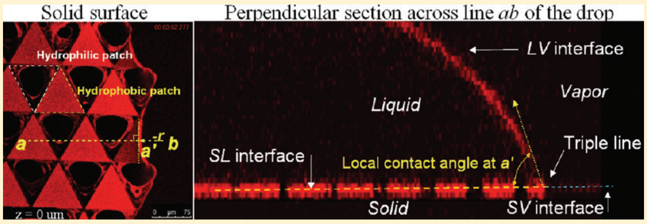

Chemical heterogeneity and physical roughness are the two key parameters of a solid which affect liquid wetting and spreading on the surface.[1] The apparent contact angle (θ^a) of a macroscopic droplet on a chemically heterogeneous but smooth solid surface can be predicted theoretically from Cassie's equation[2] or the modified Cassie equation,[3,4] and it can be measured experimentally with a contact angle goniometer.

For example, Figure 1a shows a water drop on a chemically heterogeneous surface with hydrophilic and hydrophobic patches. The apparent contact angle can be calculated by Cassie's or the modified Cassie equation or measured from a direct photograph (Figure 1b). The top of the drop is a spherical cap; however, the bottom of the drop, contacting the heterogeneous surface, is contorted. On such a surface, the local contact line and contact angle (θ^l) differ according to whether the patch is hydrophilic or hydrophobic. On a hydrophobic (hydrophilic) patch, the local contact angle is larger (smaller) due to lower (higher) surface energy, and the liquid surface is convex (concave). Although the local contact angles can be observed by microscopy from the side view, as noted above, they cannot be measured at different places. Most research has focused on the apparent contact angle[5−9] and contact line hystersis.[10−13] There is no simple theoretical model describing the relationship between a local chemical inhomogeneity or defect (size, shape, or surface property) and the consequent local contact angle. To the best of our knowledge, few experiments on local contact angle measurement have been reported to date. Pompe and Herminghaus measured the local contact angle on a stripewise wettability contrast of hydrophobic and hydrophilic domains with a periodicity from 200 to 1000 nm.[14] They used scanning force microscopy to image the topography of liquid sessile droplets with a high spatial resolution of a few nanometers. However, their method is suitable for measuring local contact angle on nanoscale heterogeneous structures. In the present study, we employed photolithography and a vapor-phase deposition technique to prepare a chemically heterogeneous solid surface with a defined hydrophobic and hydrophilic patch array with the size of 3−300 μm. We measured the local contact angles on the microscale patches by confocal microscopy and the addition of Rhodamine-B (RB) of very low concentration, from which the line tension can be derived.

The process of fabricating a hybrid solid surface with defined hydrophobic and hydrophilic patches is schematized in Figure 2a. Soda-lime glass of 1 mm thickness, used as the substrate, was cleaned with a base piranha solution (1:1:5 ammonium hydroxide, hydrogen peroxide, water) at 75 °C for 10 min, after which photoresist (PR) was patterned on the glass by photolithography. The glass was then put on a 100 °C hot plate for 1 min in order to remove residual surface moisture. 1H,1H,2H,2H-Perfluorooctyl trichlorosilane (PFOCTS) (97%; Sigma-Aldrich) subsequently was vapor-phase-deposited onto the glass for 30 min in an encapsulated chamber under about −70 kPa pressure at room temperature. For post-PFOCTS deposition, the PR was removed by acetone in an ultrasonic bath. As Figure 2a indicates, the glass surface, after its cleaning with the base piranha solution, was terminated with OH groups. Resultantly, the surfaces with PR coverage remained hydrophilic, whereas those without PR coverage became hydrophobic. We have fabricated right triangle PR patterns with different side lengths (3−300 μm). Figure 2b shows one of the PR patterns: a highlighted right triangle of 3 μm side lengths indicating the area lacking PR coverage. The patterned surface illustrated in Figure 2c was analyzed by scanning probe topographic imaging using a Seiko Instruments (Chiban, Japan) SPA300HV model atomic force microscope equipped with a titanium- and platinum-coated silicon cantilever

Received: February 23, 2011
Revised: April 19, 2011
Published: April 21, 2011

ACS Publications © 2011 American Chemical Society

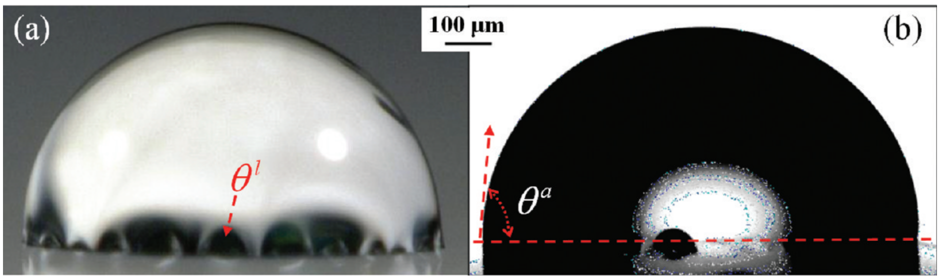

Figure 1. (a) Side view of a water drop on a heterogeneous surface with hydrophilic and hydrophobic patches. (b) Drop profile captured via a contact angle goniometer.

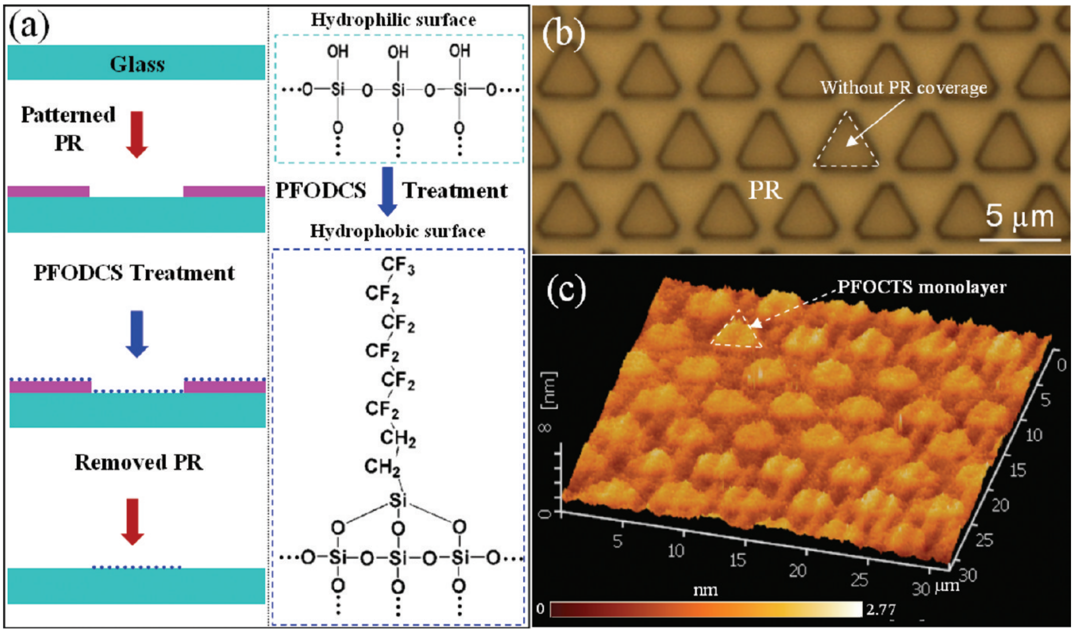

Figure 2. (a) Schematic process of fabricating a hybrid solid surface with defined hydrophobic and hydrophilic patches, and surface chemical property variation before and after PFODCS treatment. (b) PR patterns, with the highlighted right triangle of 3 μm side lengths indicating the area lacking PR coverage. (c) AFM image of the patterned surface.

(NSC3t/Ti–Pt, MikroMash) and operated in tapping mode. The triangular PFOCTS pattern was obviously higher than other areas. The average height difference, as correspondent with the PFOCTS monolayer, was 0.9 nm (roughness rms = 0.39 nm). Such a chemically heterogeneous surface is not perfectly flat, since the PFOCTS monolayer deposited onto the glass has a thickness on the order of a few angstroms. Nevertheless, its thickness is much smaller than its lateral size (ranging from several to hundreds of micrometers). Therefore, the effects of chemical heterogeneity should largely predominate over those due to the surface roughness.[1]

By mixing RB in water, we can obtain the three-dimensional structure of a water drop on the hybrid surface. Figure 3a is a 3D projection of a RB solution drop on the patterned surface (for better observation, the viewing angle is rotated). The 3D structure was obtained via a Leica TCS SP5 confocal microscope scanning parallel to glass surface (*XY* plane). To prevent evaporation, we covered the drop with a paper moistened with water. Interestingly, the RB was found to be absorbed or aggregated into both the air–liquid and solid–liquid interfaces, which can be confirmed by the contrast of fluorescent intensity shown in Figures 3b and 4a.

The inset picture in Figure 3b is one of the cross sections parallel to the *XY* plane obtained by confocal microscopic scanning (Z = 364.8 μm, the glass surface was set at Z = 0 μm). The normalized fluorescence intensity was observed as a function of distance across line ab in the inset picture. We can clearly see that the fluorescent light forms a ring shape and RB was aggregated at the ring. As pointed out in Figure 3b, the position with maximum fluorescence intensity is regarded as the position of the air–liquid interface. The liquid and the air phases are inside and outside the ring, respectively. The aggregation behavior of RB at the air–liquid interface is due to the fact that the interface is less polar than the bulk liquid.[15]

Figure 4a shows an enlarged partial cross-section of the drop (Figure 3a) focusing on the glass surface ($Z = 0$ μm). Figure 4b is a phase contrast image of Figure 4a. Comparing these two figures, their three-phase contact lines appear to be consistent. On the fluorescent image, the repeated pattern, a rhombus split into two right triangles (respectively, hydrophilic and hydrophobic patches with side lengths = 100 μm) by its diagonal, is visible. As marked in Figure 4a, the triangle with the higher fluorescent signal is the hydrophobic domain, whereas the one with the low

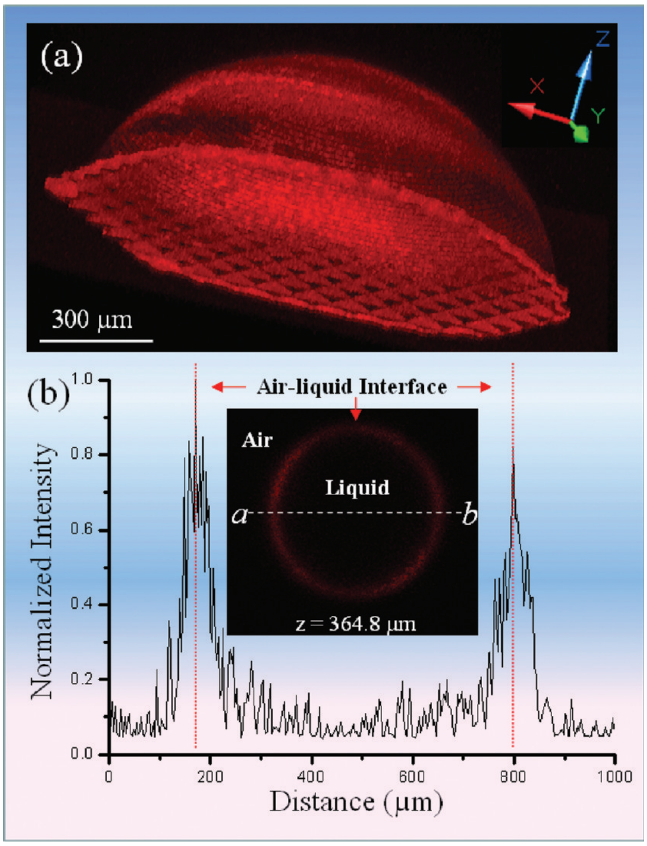

Figure 3. (a) 3D projection of a RB solution drop on the patterned surface obtained by confocal microscopy. The *XY* plane is parallel to glass surface. (b) Normalized fluorescent intensity across line ab as a function of distance, and the picture is a cross-sectional image at z = 364.8 μm.

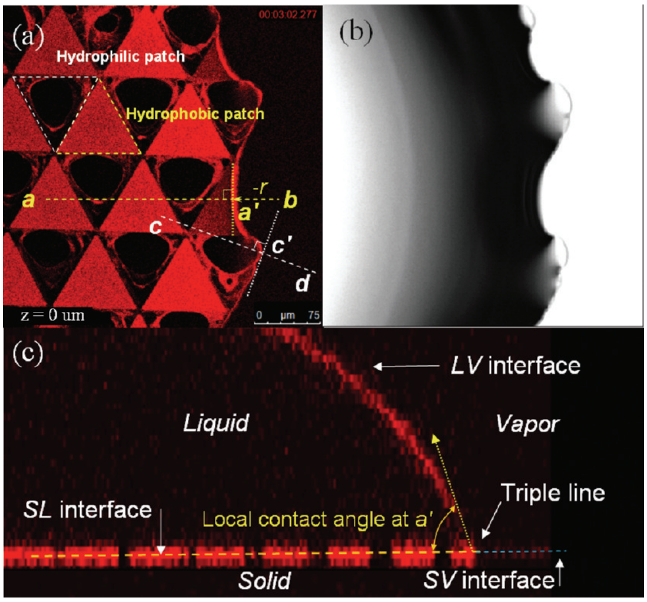

Figure 4. (a) Enlarged partial cross section of the RB solution drop focusing on the glass surface ($Z = 0$ μm). (b) Phase contrast image of (a). (c) Sectional image across line ab, L-liquid phase, V-vapor phase, S-solid phase.

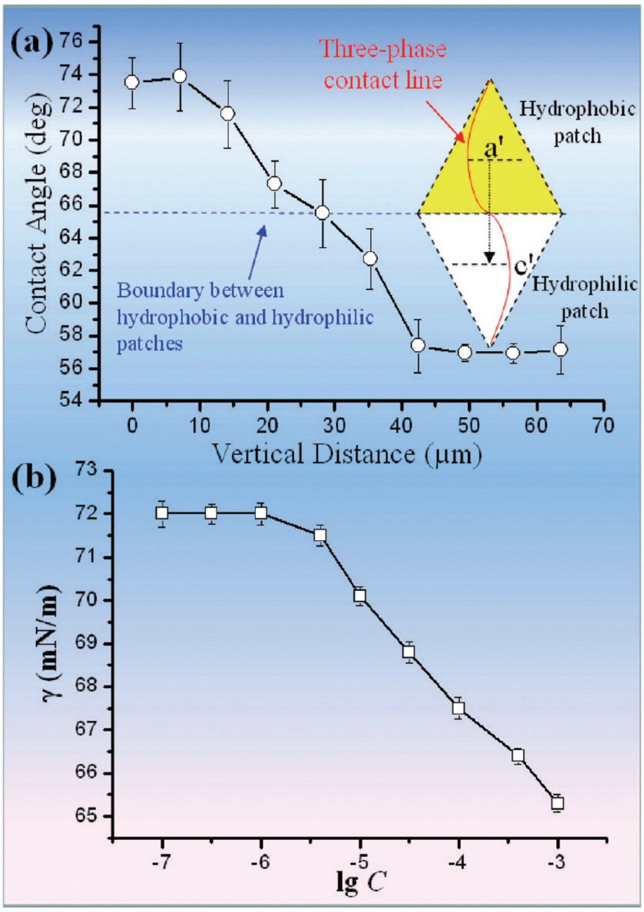

Figure 5. (a) Local contact angle as a function of vertical distance from points a′ to c′. (b) RB solution surface tension as a function of log C (concentration, mol/L).

fluorescent intensity is the hydrophilic domain. This disparity in fluorescent intensity helps to distinguish the surface properties. The RB is concentrated in the hydrophobic domain rather than the hydrophilic, since the polarity of the OH group is higher than that of the PFOCTS.

According to the definition of the contact angle, the local contact angle section should be normal to the solid surface and the three-phase contact line.[16] For example, to find the local contact angle at point a′ in Figure 4a, we first drew a tangent from the contact line and then drew another line ab vertical to this tangent through a′. Then, through ab, we sectioned the drop (Figure 3a) perpendicular to the glass surface (Figure 4a). Figures 4c presents the perpendicular section across line ab, showing the local contact angle. Three phases were found in this figure, the liquid (L), the vapor or air (V), and the solid (S), between which three interfaces are generated: the LV, the SL, and the SV. The LV and SL interfaces are considered as the positions with maximum fluorescence intensity across two phases. The extension line of the SL interface is regarded as the SV interface. These three interfaces are in contact at the triple line which is normal to the plane of Figure 4c. After analyzing Figure 4, we found the local contact angle at point a′ using a protractor.

Using this method, we measured the local contact angles from point a′ to point c′ and plotted them in Figure 5a. These angles range from 74° to 56°, in accordance with the position of the three-phase contact line. The local contact angle at the boundary between the hydrophobic and hydrophilic patches is 65.5°. The local contact angles on the hydrophobic (hydrophilic) patches increase (decrease) as they move away from the boundary or the hydrophilic (hydrophobic) patch. The contact angles reach a peak value or plateau as they approach another hydrophilic (hydrophobic) patch.

The apparent contact angle (θ^a) satisfies the modified Young's equation, which includes the line tension[17]

$$\gamma_{SV_i} - \gamma_{SL_i} = \gamma_{LV_i} \cos \theta_i^a + \frac{\gamma_{SLV_i}}{r_i} \qquad (2)$$

where γ_{SV}, γ_{SL}, and γ_{LV} are the interfacial tensions for solid/vapor, solid/liquid and liquid/vapor interfaces, respectively, r is the radius of curvature of the three-phase contact line at a local position, and γ_{SLV} is the line tension.

Meanwhile, the local contact angle (θ^l) satisfies the Young's equation[18]

$$\gamma_{SV_i} - \gamma_{SL_i} = \gamma_{LV_i} \cos \theta_i^l \qquad (3)$$

and at the same point, we have

$$\gamma_{SV_i} - \gamma_{SL_i} = \gamma_{LV} \cos \theta_i^a + \frac{\gamma_{SLV_i}}{r_i} = \gamma_{LV} \cos \theta_i^l \qquad (4)$$

$$\gamma_{SLV_i} = \gamma_{LV} \left(\cos \theta_i^l - \cos \theta_i^a \right) r_i \qquad (5)$$

The line tension γ_{SLV} can be derived from eq 5 if γ_{LV}, θ^l, θ^a, and r are given. We measured the surface tensions of different concentrations of RB solution by the Wilhelmy plate method (Langmuir–Blogett trough, Nima), and the corresponding data are plotted in Figure 5b as $\gamma - \log C$. From the curve, we can see that the surface tension does not decrease until the RB concentration is higher than 1×10^{-6} mol/L. Here, we used 2×10^{-7} mol/L RB solution for the local contact angle measurement. The apparent contact angles of the RB solution on glass and PFOCTS-treated glass are 13.5° and 99.1°, respectively, the same as those for deionized water. Using the local contact angle measured by confocal microscopy, we found the line tension to be $(-2.06-1.53) \times 10^{-6}$ J/m, which is in the same order of magnitude as those measured by other methods.[19−21] Note that the normal vector of curvature is from the inside to the outside of the three-phase contact line which is a closed curve. Thus, the negative line tension was found here. However, from the time the concept of line tension was first postulated by Gibbs more than 100 years ago, divergent values have been reported by various authors. These values vary from 3×10^{-12} to over 1×10^{-5} J/m; moreover, the sign of the line tension is also controversial.[22] In this light, measuring the local contact angle could represent a better means of understanding line tension and the parameters affecting its magnitude and sign. The current limitation, the indistinguishableness of local contact angles on such a hybrid surface with pattern sizes smaller than 5 μm, can be eliminated by increasing the RB concentration. We measured the local contact angle with the protractor in ImageJ software with the naked eye. Although the protractor provides 0.001° precision, the precision of our method depends on drawing the tangent of the LV interface. In fact, the resolution of the cross section (Figure 4c) affects the determination of local contact angle. The clearer the cross section, the easier and more precise it is to find the tangent of the LV interface. We repeated the steps and found that the precision is ±2° with the Leica TCS SP5 confocal microscope.

In conclusion, we demonstrate a simple approach for measuring the local contact angle of a liquid drop spreading on a heterogeneous solid surface with hydrophobic and hydrophilic patch, specifically by confocal microscopy and the addition of a very low concentration of RB (2×10^{-7} mol/L). RB at that concentration was found to be absorbed at the air–liquid and solid–liquid interfaces and thus did not affect the properties of bulk-phase water (surface tension and contact angle). This adsorptive behavior helps us to distinguish liquid and solid surfaces as well as hydrophobic and hydrophilic patches by their corresponding fluorescent intensities. Additionally, this method can be used to measure the local contact angle under the influence of physical roughness.

■ AUTHOR INFORMATION

Corresponding Author

*E-mail: phwen@ust.hk.

■ ACKNOWLEDGMENT

This publication is based on work partially supported by Award No. SA-C0040/UK-C0016, made by King Abdullah University of Science and Technology (KAUST), Hong Kong RGC grants HKUST 603608 and 604710, respectively.

■ REFERENCES

(1) Bonn, D.; Eggers, J.; Indekeu, J.; Meunier, J. *Rev. Mod. Phys.* **2009**, *81*, 739.
(2) Cassie, A. B. D. *Discuss. Faraday Soc.* **1948**, *3*, 11.
(3) Drelich, J.; Miller, J. D. *Langmuir* **1993**, *9*, 619.
(4) Drelich, J.; Wilbur, J. L.; Miller, J. D.; Whitesides, G. M. *Langmuir* **1996**, *12*, 1913.
(5) Gupta, P.; Ulman, A.; Fanfan, S.; Korniakov, A.; Loos, K. *J. Am. Chem. Soc.* **2005**, *127*, 4.
(6) Polster, D.; Graaf, H.; Baumgärtel, T.; Von Borczyskowski, C.; Benedikt, U.; Auer, A. A. *Langmuir* **2010**, *26*, 8301.
(7) Larsen, S. T.; Taboryski, R. *Langmuir* **2009**, *25*, 1282.
(8) Drelich, J. *Pol. J. Chem.* **1997**, *71*, 525.
(9) de Jonghe, V.; Chatain, D. *Acta Metall. Mater.* **1995**, *43*, 1505.
(10) Kalinin, Y. V.; Berejnov, V.; Thorne, R. E. *Langmuir* **2009**, *25*, 5391.
(11) Nadkarni, G. D.; Garoff, S. *Europhys. Lett.* **1992**, *20*, 523.
(12) Cubaud, T.; Fermigier, M. *J. Colloid Interface Sci.* **2004**, *269*, 171.
(13) Schwartz, L. W.; Garoff, S. *Langmuir* **1985**, *1*, 219.
(14) Pompe, T.; Herminghaus, S. *Phys. Rev. Lett.* **2000**, *85*, 1930.
(15) Zheng, X. -.; Harata, A.; Ogawa, T. *Spectrochim. Acta, Part A* **2001**, *57*, 315.
(16) De Gennes, P. G. *Rev. Mod. Phys.* **1985**, *57*, 827.
(17) Boruvka, L.; Neumann, A. W. *J. Chem. Phys.* **1977**, *66*, 5464.
(18) Young, T. *Philos. Trans. R. Soc. London* **1805**, *95*, 65.
(19) Chen, P.; Susnar, S. S.; Amirfazli, A.; Mak, C.; Neumann, A. W. *Langmuir* **1997**, *13*, 3035.
(20) Gaydos, J.; Neumann, A. W. *J. Colloid Interface Sci.* **1987**, *120*, 76.
(21) Li, D.; Neumann, A. W. *Colloids Surf.* **1990**, *43*, 195.
(22) Drelich, J. *Colloids Surf., A* **1996**, *116*, 43.